THEORETICA CHIMICA ACTA

Theoret. Chim. Acta (Berl.) 61, 73–85 (1982)

Applicability of Momentum Density Approach

Toshikatsu Koga and Mutsuo Morita

Departments of Industrial Chemistry and of Applied Science for Energy, Muroran Institute of Technology, Muroran, Hokkaido 050, Japan

Using the Nelander's form of the virial theorem and its further modification, we show that the method of momentum electron density proposed previously for uniform scaling processes of polyatomic systems is applicable to a wide range of nuclear rearrangement problems, in which bond lengths or bond angles may concern in a complicated way. The use of experimental Compton profile is also mentioned as a basic quantity in this approach. The present development is illustrated by an application of the method to the bending process in a triatomic system.

Key words: Momentum density – Compton profile – Virial theorem – Nuclear rearrangement process.

1. Introduction

In a previous paper [1], we have proposed a method of momentum electron density which permits to clarify the origin of nuclear rearrangements, such as molecular geometries and chemical reactions, in terms of the concept in momentum ($p-$) space instead of the usual one in coordinate ($r-$) space. The approach has been motivated by the fact of equivalent ability of the two variables, position r and momentum p, in describing quantum-mechanical systems [2]. Applying the ordinary virial theorem (see e.g. [3]) to a uniform scaling process [4–6] such as a totally symmetric stretching mode, we have derived three sets of rigorous expressions for total energy and its gradient of a polyatomic system using the momentum electron density $\rho(\mathbf{p})$ as a basic physical quantity. It has been then suggested that the contractive and expansive behaviours of $\rho(\mathbf{p})$ form an important guiding principle in understanding and predicting the nature of nuclear rearrangements in p-space.

0040-5744/82/0061/0073/$02.60

Furthermore, we have recently shown [7] that a rigorous relation between the energy and the momentum density can also be deduced from the integrated Hellmann–Feynman theorem with respect to the electron mass [8, 9], and that the relation is also applicable to the study of nuclear isotope effect if the nuclear mass, instead of the electron mass, is taken as a parameter.

The proposed method of momentum density has been applied to the $\sigma(1s\sigma_g$ and $2p\sigma_u)$ and $\pi(2p\pi_u$ and $3d\pi_g)$ states of H_2^+ system, and the processes of these attractive and repulsive interactions have been analyzed in detail based on the behaviour of momentum density [10, 11]. In these studies, it has been clarified that the required density information can be reduced from the three-dimensional $\rho(\mathbf{p})$ to the one-dimensional radial momentum density $I(p)$ without loss of generality and exactness of the approach [10]. Parallelism between the behaviours of $I(p)$ and Compton profile $J(q)$ has also been pointed out [11].

The purpose of this paper is to extend the applicability of the momentum density approach to processes other than the uniform scaling. Using the Nelander's form [12] of the virial theorem and its further modification, we show that the approach can be applied to various kinds of nuclear rearrangement processes including, for example, the bending and antisymmetric-stretching processes in molecular geometries and the formation and breaking processes of several bonds in chemical reactions. In this development, no approximations are introduced and the exactness of our basic equations are preserved. The guiding principle of contraction and expansion for the behaviour of momentum density is also valid. The difference of the present treatment from the previous one for the uniform scaling is that the optimization of several internal coordinates is newly required. We also show that all the basic equations in our approach can be rewritten by using the experimentally-observed Compton profile $J(q)$ (see [13–15] for reviews) as a fundamental physical quantity. The same guiding principle holds for the behaviour of $J(q)$ as for those of $\rho(\mathbf{p})$ and $I(p)$. Consequently, either of $\rho(\mathbf{p})$, $I(p)$, or $J(q)$ is shown to be an acceptable quantity in constructing and developing the momentum density approach.

These theoretical developments are presented in the next section. The results are illustrated in Sect. 3 for the bending process in a triatomic system.

2. Applicability of Momentum Density Approach

2.1. Uniform Scaling Process

For the sake of later reference, we here outline the derivation of basic equations of the momentum density approach for uniform scaling processes [1].

The polyatomic virial theorem in ordinary form [3]

$$T(\mathbf{R})+E(\mathbf{R})+\sum_A \mathbf{R}_A[\partial E(\mathbf{R})/\partial \mathbf{R}_A]=0 \tag{1}$$

with T and E being the kinetic and total energies, respectively, and $\mathbf{R}\equiv\{\mathbf{R}_A\}$

the nuclear coordinates is reduced to [4–6]

$$T(s)+E(s)+s[dE(s)/ds]=0, \tag{2}$$

if we consider a uniform scaling process $\mathbf{R}=s\mathbf{R}_0$ of an arbitrary reference conformation $\mathbf{R}_0$. The scale factor s varies from 0 (united atom limit) to ∞ (separated atoms limit). Solving Eq. (2) and using $T(s)=\int d\mathbf{p}(p^2/2)\rho(\mathbf{p};s)$, we obtain three formulas which rigorously connect E with $\rho(\mathbf{p})$,

$$E(s)=\int d\mathbf{p}\,(p^2/2)\left\{(1/s)\int_s^\infty ds'\,[\rho(\mathbf{p};s')-\rho(\mathbf{p};\infty)]-\rho(\mathbf{p};\infty)\right\}, \tag{3a}$$

$$E(s)=\int d\mathbf{p}(p^2/2)\left\{-(1/s)\int_0^s ds'\,\rho(\mathbf{p};s')\right\}+V_{nn}(s), \tag{3b}$$

$$E(s)=\int d\mathbf{p}\,(p^2/2)\left\{(1/s)\int_s^{s_e} ds'\,\rho(\mathbf{p};s')-(s_e/s)\rho(\mathbf{p};s_e)\right\}, \tag{3c}$$

where $\mathbf{p}$ stands for the momentum vector of an electron, $p=|\mathbf{p}|$, and V_{nn} the nuclear repulsion potential. Eqs. (3b) and (3c) are obtained respectively by imposing the kinetic field normalization condition ($\int_0^\infty ds'\,[T(s')-T(\infty)]=sV_{nn}(s)$) [5] and the equilibrium condition ($dE/ds|_{s=s_e}=0$) on Eq. (3a). The corresponding expressions for the force F are immediately obtained as a function of $\rho(\mathbf{p})$ by the definition $F\equiv -dE/ds$. These basic equations can also be deduced from the integrated Hellmann–Feynman theorem with respect to the electron mass [7].

The three Eqs. (3a–c) are characterized by the range of integration about the scale parameter s. They are respectively convenient to investigate the interaction process starting from the separated atoms (Eq. (3a)), the change from the united atom (Eq. (3b)), and the change around the equilibrium conformation (Eq. (3c)). Note that in Eqs. (3a) and (3c), the contribution of V_{nn} is implicitly included in the integral term of $\rho(\mathbf{p})$.

2.2. Other Processes: Present Development

The reduction of the polyatomic virial theorem (1) to Eq. (2) occupies a crucial step in formulating our method of momentum density. For general processes of nuclear rearrangements other than the uniform scaling, it seems difficult to simplify Eq. (1) to the form of Eq. (2). Therefore, we start from the Nelander's form [12] of the virial theorem instead of the ordinary form (1). This treatment enables us to generalize the momentum density approach to various rearrangement problems. The uniform scaling process is included as a special case.

The polyatomic virial theorem of Nelander [12] is given by

$$T(\mathbf{R},\boldsymbol{\theta})+E(\mathbf{R},\boldsymbol{\theta})+\sum_{i=1}^{n} R_i[\partial E(\mathbf{R},\boldsymbol{\theta})/\partial R_i]=0, \tag{4}$$

where $\{\mathbf{R},\boldsymbol{\theta}\}$ are the minimal set of internal coordinates consisting of bond lengths $\mathbf{R}=\{R_1, R_2, \ldots, R_n\}$ and bond angles $\boldsymbol{\theta}=\{\theta_1, \theta_2, \ldots, \theta_m\}$ which are sufficient to

specify the conformation of a given molecular system. When $m=0$ and there are no angular variables, Eq. (4) becomes the Parr–Brown form [16] of the virial theorem.

By imposing some conditions, Eq. (4) can be reduced to simpler forms tractable in our approach. In the following, we discuss two of such methods of reduction, which are referred to as *Methods* (A) and (B).

Method (A). Treat the bond length R_j under consideration as an independent variable and optimize the other bond lengths $\{R_i\}$ $(i \neq j)$ so that the total energy is extremum for a given R_j. Since $\partial E/\partial R_i|_{R_i=R_i^0}=0$ $(i \neq j)$, Eq. (4) then takes the form of Eq. (2);

$$T(R_j)+E(R_j)+R_j[dE(R_j)/dR_j]=0, \tag{5}$$

where $T(R_j)$ and $E(R_j)$ respectively denote $T(R_j;\{R_i^0\},\boldsymbol{\theta})$ and $E(R_j;\{R_i^0\},\boldsymbol{\theta})$. Replacing s with R_j, we can therefore apply all the basic equations (3a–c) to this R_j-path. Note that in some cases the range of R_j value may be different from that of the scale factor s, $[0,\infty)$, and modification may be needed for the region of integration.

When there is only one bond length in the employed set of internal coordinates, the above-mentioned procedure of optimization is unnecessary and this bond length R play an equivalent role as the scale factor s. Namely, *Method* (A) includes the treatment for uniform scaling processes as a special case of $n=1$.

Some of nuclear rearrangement problems to which the momentum density approach becomes applicable by *Method* (A) are (a) stretching of a particular bond, (b) change in bond angle (by examining the length R_{AC} corresponding to the angle $<ABC$), (c) change in out-of-plane angle and internal rotation (by examining some relevant length as in (b)), (d) reaction process whose reaction coordinate is a formation (or breaking) of a particular bond, and (e) long-range and van der Waals forces.

Method (B). For a given set of angles $\boldsymbol{\theta}$, optimize all bond lengths R so that $\partial E/\partial R_i|_{R_i=R_i^0}=0$. Then the virial theorem (4) takes its simplest form,

$$E(\boldsymbol{\theta};\mathsf{R}^0)=-T(\boldsymbol{\theta};\mathsf{R}^0), \tag{6a}$$

and the energy-momentum density relation is given by

$$E(\boldsymbol{\theta})=-\int d\mathsf{p}\,(p^2/2)\rho(\mathsf{p};\boldsymbol{\theta}), \tag{6b}$$

as in the atomic case.

Since the energy is given as a function of bond angles, this method may be useful to study the angular problem in molecular geometries (see e.g. (b) and (c) of the above discussion). The method can also be applied to intra-molecular rearrangement reactions such as $ABC \rightarrow CAB$ by treating the angle $<ABC$ as a reaction coordinate.

When compared with *Method* (*A*), *Method* (*B*) has the advantage that the latter does not include the integral terms like $\int ds\,\rho(\mathsf{p}; s)$. In *Method* (*B*), however, the force F is not represented by the momentum density $\rho(\mathsf{p}; \boldsymbol{\theta})$, but requires its gradient $\partial\rho(\mathsf{p}; \boldsymbol{\theta})/\partial\theta_i$.

Eq. (6), as well as Eqs. (3a) and (3c), implicitly includes the contribution of the nuclear repulsion potential. Furthermore, these equations constitute additive partitionings of the total energy E into orbital components within the framework of independent particle models. Based on this characteristic of Eq. (6), Takahata and Parr [17] gave a re-examination of the Walsh rule [18] for H_2O molecule using the orbital kinetic energies.

The simplification by *Methods* (*A*) and (*B*) is also valid for the cases where bond lengths R and bond angles $\boldsymbol{\theta}$ are not explicit variables. Let us consider a linear transformation of coordinates, $(R_1, R_2, \ldots, R_n) \rightarrow (S_1, S_2, \ldots, S_n)$ and $(\theta_1, \theta_2, \ldots, \theta_m) \rightarrow (S_{n+1}, S_{n+2}, \ldots, S_{n+m})$, where the variables R and $\boldsymbol{\theta}$ are assumed to be transformed without mixing. Examples of the new coordinates S may be found in symmetry and normal coordinates. After some manipulation, we obtain a modification of Eq. (4),

$$T(\mathsf{S}) + E(\mathsf{S}) + \sum_{i=1}^{n} S_i[\partial E(\mathsf{S})/\partial S_i] = 0, \tag{7}$$

which is again a form subject to the application of *Methods* (*A*) and (*B*). By the use of this modified virial theorem (7), the momentum density approach further extends its applicability to the problem of nuclear rearrangements in which several bonds or angles concern through a coordinate S_i. The antisymmetric stretching in the molecular vibration is a simple example of this extended applicability.

Thus, we see that the approach of momentum density applies not only to the uniform scaling process but also to various kinds of nuclear rearrangement processes where several bond lengths or bond angles may participate in a complex manner. The virial theorem in the Nelander's form (Eq. (4)) and its further modification (Eq. (7)) have been essential in this development.

2.3. Compton Profile as a Basic Quantity

Previously [10], it has been shown that the density information required in the basic Eqs. (3a–c) and (6b) is reducible from the three-dimensional $\rho(\mathsf{p})$ to the one-dimensional radial momentum density $I(p)$,

$$I(p) = p^2 \int_0^{2\pi} d\phi_p \int_0^{\pi} d\theta_p \sin\theta_p \rho(\mathsf{p}), \tag{8}$$

since the kinetic energy operator $(p^2/2)$ appearing in these equations is angular-independent. For example, Eq. (3a) is rewritten as

$$E(s) = \int_0^{\infty} dp\,(p^2/2)\left\{(1/s)\int_s^{\infty} ds'\,[I(p; s') - I(p; \infty)] - I(p; \infty)\right\}. \tag{9a}$$

We here point out that the Compton profile $J(q)$, which may be observed experimentally, is also acceptable as a basic physical quantity in our approach. Under the impulse approximation [13–15], $I(p)$ and $J(q)$ are related as

$$J(q) = (1/2) \int_{|q|}^{\infty} dp\, p^{-1} I(p), \tag{10a}$$

$$I(p) = -2p[dJ(p)/dp]. \tag{10b}$$

Therefore, we immediately obtain an integral equality

$$\int_0^{\infty} dp\, (p^2/2) I(p) = \int_0^{\infty} dp\, (3p^2) J(p), \tag{11}$$

which can be directly used to rewrite the basic equations in a reduced form (Eq. (9a) and its analogues). Eq. (9a), for instance, becomes

$$E(s) = \int_0^{\infty} dp\, (3p^2) \left\{ (1/s) \int_s^{\infty} ds' \, [J(p; s') - J(p; \infty)] - J(p; \infty) \right\}. \tag{9b}$$

The relation (11) was also used by Coulson [19] who discussed the definition of bond energy based on the approximate additivity of Compton profile.

Examination of the behaviour of $J(q)$ and its contributions to E and F shows that the same guiding principle of contraction and expansion, as that for $\rho(\mathsf{p})$ and $I(p)$ [1, 10], holds for $J(q)$. Parallelism between the behaviours of $I(p)$ and $J(q)$ has already been observed in the study of the H_2^+ system [11]. Consequently, either of $\rho(\mathsf{p})$, $I(p)$, or $J(q)$ may be employed to construct the method of momentum density. The experimental nature of $J(q)$ and its close connection to $I(p)$ and $\rho(\mathsf{p})$ suggest the possibility of experimental verification of this approach in some cases.

3. Illustration: Bending Process in a Triatomic System

As an application of the momentum density approach to processes other than the uniform scaling, we here discuss the bending process in a triatomic system. The simplest triatomic system H_3^{2+} is unstable than the separated atoms and does not form a molecule (see e.g. [20]). We therefore give an illustrative treatment for a hypothetical one-electron system where three nuclei have charge of $+\frac{1}{2}$.

The r-space wavefunction of the system is approximated by a linear combination of one-term Gaussian AOs of $1s$ type. That is

$$\Psi(\mathsf{r}) = c_1\chi_1(\mathsf{r}) + c_2\chi_2(\mathsf{r}) + c_3\chi_3(\mathsf{r}), \tag{12a}$$

$$\chi_i(\mathsf{r}) = (2\zeta/\pi)^{3/4} \exp(-\zeta|\mathsf{r} - \mathsf{R}_i|^2), \qquad (i = 1, 2, 3) \tag{12b}$$

where R_i denotes the position of ith nucleus and the exponent ζ is optimized so as to minimize the energy of the system for every nuclear conformation. Under this approximation, the energy surface for isosceles conformations is

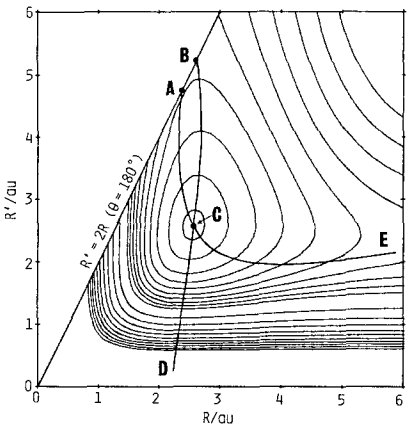

Fig. 1. Energy surface and bending paths. Contour values are -0.243, $-0.24(0.005)-0.2(0.02)0$ from the innermost line. The (R, R') bending path is given by BCD, while the (R, θ) bending path by ACE. The point C means equilibrium conformation. All values in atomic units

depicted in Fig. 1, where R means the length of two equal bonds and R' the length of the remnant which corresponds to the bond angle θ. The system is shown to have an equilateral equilibrium with $R = R' = 2.5627$ a.u. Fig. 1 resembles the energy map for H_3^+ system [21], and we may expect some similarity for the behaviours of momentum density of the two systems.

The isosceles geometries are specified by a set of two internal coordinates. The (R, R') and (R, θ) coordinates, to which *Methods* (A) and (B) apply respectively, are examined here. Depending on this choice, the bending paths are different. In the (R, R') coordinates, the bending path satisfying the condition $\partial E(R, R')/\partial R = 0$ is given by the curve BCD in Fig. 1, while in the (R, θ) coordinates the path satisfying $\partial E(R, \theta)/\partial R = 0$ is given by the curve ACE. The two curves pass through the equilibrium point C, but they differ remarkably in the region of small bond angles.

The momentum electron density of this system is obtained as follows. The Dirac–Fourier transform [2, 22] of Eq. (12) yields the p-space wavefunction,

$$\Psi(\mathbf{p}) = c_1\chi_1(\mathbf{p}) + c_2\chi_2(\mathbf{p}) + c_3\chi_3(\mathbf{p}), \tag{13a}$$

$$\chi_i(\mathbf{p}) = \{\exp(-i\mathbf{p}\mathbf{R}_i)\}\{(2\pi\zeta)^{-3/4}\exp(-p^2/4\zeta)\}. \tag{13b}$$

The momentum density is then given by

$$\rho(\mathbf{p}) = \{c_1^2 + c_2^2 + c_3^2 + 2c_1c_2\cos[\mathbf{p}(\mathbf{R}_1 - \mathbf{R}_2)] + 2c_2c_3\cos[\mathbf{p}(\mathbf{R}_2 - \mathbf{R}_3)] + 2c_3c_1\cos[\mathbf{p}(\mathbf{R}_3 - \mathbf{R}_1)]\}\{(2\pi\zeta)^{-3/2}\exp(-p^2/2\zeta)\}, \tag{14}$$

and the radial density is found to be

$$I(p) = \{c_1^2 + c_2^2 + c_3^2 + 2(c_1c_2 + c_2c_3)\sin(Rp)/Rp + 2c_3c_1\sin(R'p)/R'p\} \times \{(2/\pi\zeta^3)^{1/2}p^2\exp(-p^2/2\zeta)\}, \tag{15}$$

after the integration about the angular variables. Eq. (15) is given in the (R, R') coordinates, and in the (R, θ) coordinates R' should be replaced with $2R\sin(\theta/2)$.

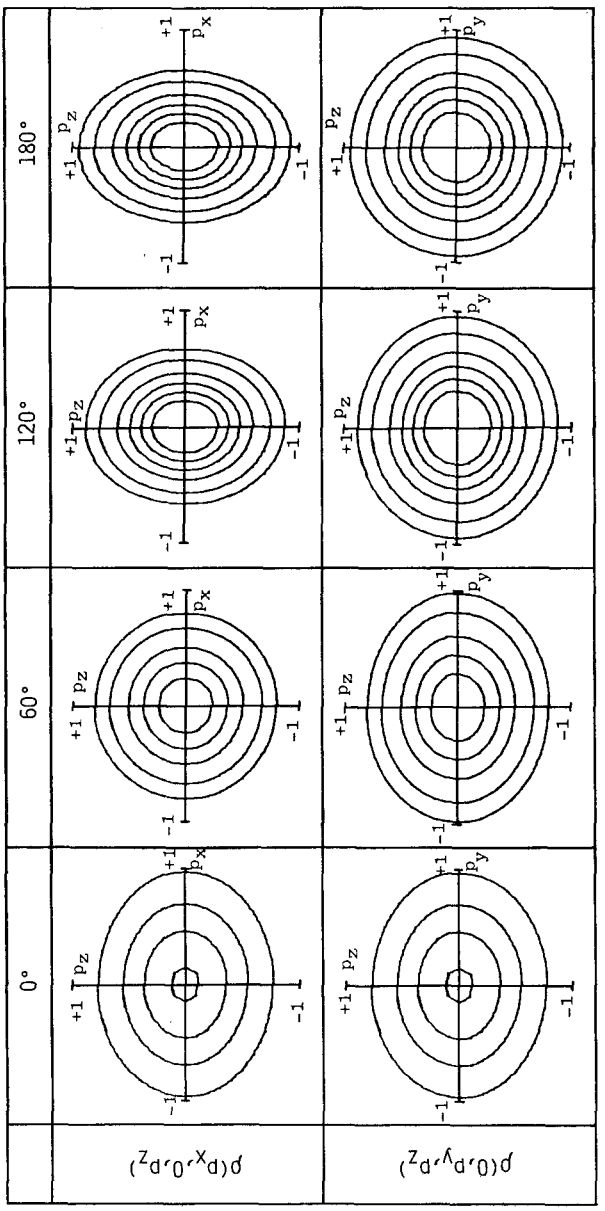

Fig. 2. Profiles of momentum density distribution as a function of bond angle. Contour values are 0.1, 0.2(0.2)1.0 in atomic unit from the outermost line. For the maps of 0°, contour of 0.3 a.u. is added

Fig. 2 shows typical profiles of $\rho(\mathrm{p})$ at several points on the path *BCD*. The p-space axes (p_x, p_y, p_z) are taken to be parallel to the r-space axes (x, y, z), which have been so chosen that the z-axis is the C_{2v} axis and the x- and y-axes are respectively in and normal to the molecular plane. As the bond angle decreases from 180° (linear form), the distribution $\rho(p_x, 0, p_z)$ parallel to the molecular plane changes from an ellipse with vertical major axis (180° and 120°), via a circle (60°), to an ellipse with horizontal major axis (0°). (The angle of 0° means the diatomic limit where the two terminal nuclei are united to a single one.) This behaviour implies that the kinetic pressure gradually increases in the p_x direction, and reflects the change in the coordinate density $\rho(\mathrm{r})$, which initially has major distribution along the x axis but finally does along the z axis. The distribution $\rho(0, p_y, p_z)$ perpendicular to the molecular plane reveals a monotonous change from a circle (180°) to an ellipse (120°–0°). This corresponds to a decrease of the space of electronic motion in the y direction with a concomitant increase in the y component of kinetic energy. In both densities, $\rho(p_x, 0, p_z)$ and $\rho(0, p_y, p_z)$, considerable expansion is noticeable at 0° when compared to 180°.

In the following, these behaviours of momentum density are quantitatively examined along the two bending paths, together with their contributions to the energy and force of the system.

3.1. (R, R') Bending Process

Referring the density of the linear conformation, the change in radial momentum density $\Delta I[\equiv I(R') - I(R' = 2R)]$ is shown in Fig. 3a along the bending path *BCD*. For simplicity, this and succeeding plots are given as a function of bond angle which results from the conversion relation $\theta = 2 \arcsin(R'/2R)$. As the bond angle decreases, the ΔI plot initially shows contraction (150° and 120°)

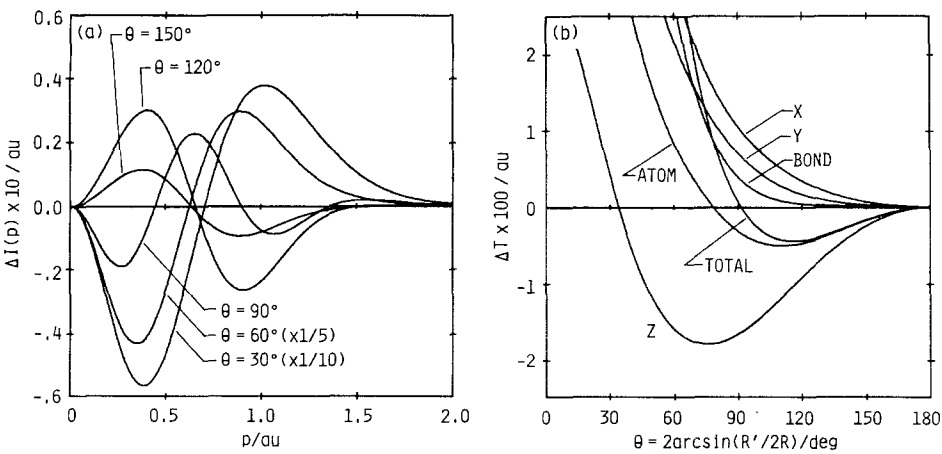

Fig. 3. The (R, R') bending process. (a) The density difference ΔI and (b) the resultant kinetic energy ΔT as a function of the converted bond angle $\theta = 2 \arcsin(R'/2R)$

and changes to expansion at 60° and 30°. For 90°, ΔI has a critical nature between them. Correspondingly, ΔT given in Fig. 3b (see the total curve) is negative for $\theta > 90°$ and positive for $\theta < 90°$. According to the guiding principle [1], these changes in ΔI (and hence ΔT) predict the existence of a stable equilibrium at $\theta < 90°$. Decomposition of ΔI and ΔT into additive components [1, 10] clarifies the origin of this behaviour. (The results are shown only for ΔT.) In the directional partitioning, the z component is a predominant origin of negative ΔT. This is a direct reflection of the enlargement of the space of electron movement in this direction as the bond angle decreases (see also Fig. 2). In the atom-bond partitioning, the atomic contribution is larger, since the kinetic pressure lowers in this portion as the density flows from the one-center atomic to the two-center bond part.

The modified density difference $\Delta\bar{I}[\equiv(1/R')\int_{R'}^{R'=2R} dR'\{I(R')-I(R'=2R)\}]$ is depicted in Fig. 4a, which corresponds to the stabilization energy ΔE[1]. All the required integrations have been numerically carried out using the Gauss formula. As θ decreases, the contraction of $\Delta\bar{I}$ increases and at 60° it reaches maximum. After this, the degree of contraction decreases (e.g. 40°) and at 30° $\Delta\bar{I}$ changes to expansion. As a result, the total curve for ΔE (Fig. 4b) shows stabilization of the system and is minimum at $\theta = 60°$ (equilibrium conformation). The presence of this equilibrium is in accord with the prediction from ΔI. Similar to the case of ΔT, the partitioning into components shows the importance of the z and atomic parts.

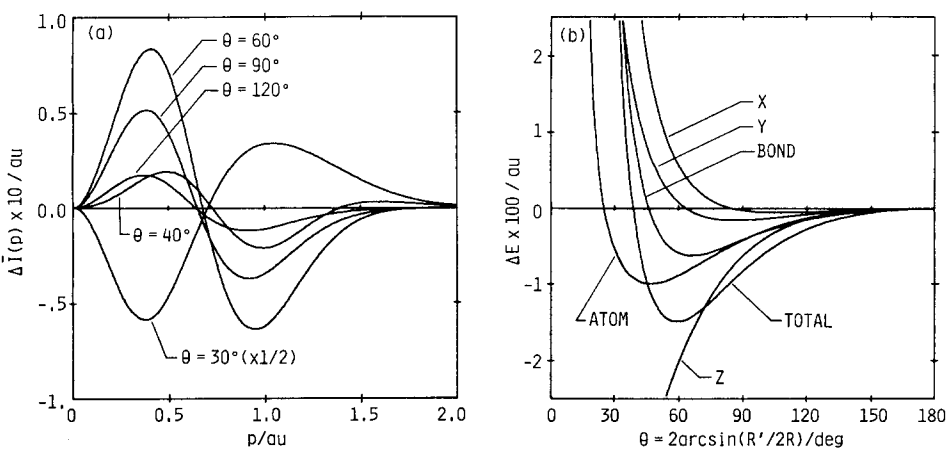

Fig. 4. The (R, R') bending process. (a) The modified density difference $\Delta\bar{I}$ and (b) the resultant stabilization energy ΔE as a function of the converted bond angle $\theta = 2\arcsin(R'/2R)$

1. In the (R, R') bending path, $T+E$ does not vanish at the reference linear geometry (the point B in Fig. 1). Therefore, the evaluation of ΔI and its components requires simple modification of the original method which is attained by taking a preliminary reference point where $T+E=0$ (the point A in the present case). From the same reason, the force is not zero at the point B (see Fig. 5b).

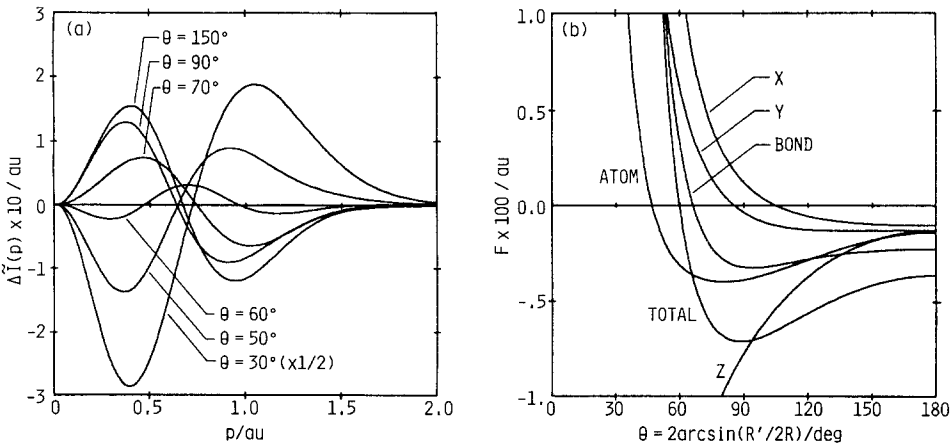

Fig. 5. The (R, R') bending process. (a) The modified density difference $\Delta\tilde{I}$ and (b) the resultant force F as a function of the converted bond angle $\theta = 2 \arcsin (R'/2R)$

Fig. 5 shows the modified difference $\Delta\tilde{I}[\equiv \Delta I + \Delta\bar{I}]$ and the resultant force F. In accordance with the guiding principle, the correspondence is clearly observed between the contraction and expansion of $\Delta\tilde{I}$ and the attraction and repulsion in F. A critical behaviour is also seen for $\theta = 60°$ where $F = 0$.

Based on *Method* (A), we are thus able to treat the bending process in a triatomic system in the same manner as the problem of diatomic interactions [10, 11]. The guiding principle is valid and common to both processes of nuclear rearrangements with the same physical picture.

3.2. (R, θ) Bending Process

In the (R, θ) coordinates, $-\Delta I$ governs $\Delta E (= -\Delta T)$ by the relation (6) of *Method* (B). Fig. 6 shows the plots for $-\Delta I$ along the path ACE together with the results for ΔE. With the decrease in θ, $-\Delta I$ increases its contraction with a maximum at $\theta = 60°$. For $\theta < 60°$, the degree of contraction decreases rapidly, and the expansion is observed at $\theta = 30°$. The total curve for ΔE shows stabilization of the system with the progress of bending, reaching the equilibrium conformation of 60°. We thus see that the guiding principle for the $\Delta\bar{I} - \Delta E$ relation in *Method* (A) directly applies to $(-\Delta I) - \Delta E$ relation in *Method* (B). The density differences $\Delta\bar{I}$ and $-\Delta I$ in the two methods show a parallel behaviour and play a similar role during the two bending processes (compare Figs. 4a and 6a). In Fig. 7, the change of Compton profile is given along the (R, θ) path. It clearly shows the behaviours of contraction and expansion corresponding to those of ΔI (Fig. 6a) and yields the ΔE curve identical to that obtained from ΔI (Fig. 6b). As discussed in Sect. 2.3, this exemplifies the utility of Compton profile as a basic physical quantity of this approach under the same guiding principle.

However, the results for the energy partitionings (Fig. 6b) are quite different from those of the (R, R') coordinates (Fig. 4b). In the directional partitioning,

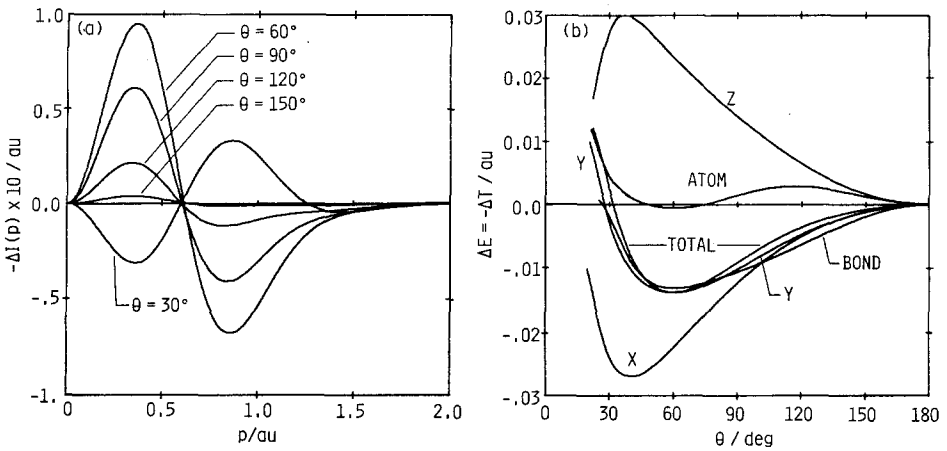

Fig. 6. The (R, θ) bending process. (a) Negative of the density difference ΔI and (b) the resultant $\Delta E = -\Delta T$ as a function of the bond angle θ

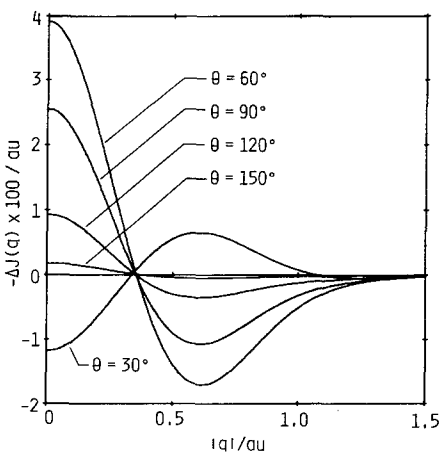

Fig. 7. The (R, θ) bending process. Negative of the Compton profile difference ΔJ as a function of the bond angle θ

the x and y parts contribute to stabilization, while the z component contributes to destabilization. Moreover, the negative x and positive z parts nearly cancel each other, and hence the y component well overlaps with the total curve. In the atom–bond partitioning, the atomic contribution is very small and the bond part is almost parallel to the total curve.

The assignments of the predominant origin for the stabilization in the bending process are just reversed in *Methods* (A) and (B). This is attributed to the anti-parallelism between the behaviours of ΔT and ΔE in *Method* (B). In the latter method, ΔE is parallel to ΔV (change in potential energy), since $\Delta E = -\Delta T = (1/2)\Delta V$. Therefore the r-space picture from the parallel component ΔV seems to be more intuitive than the p-space picture from the anti-parallel component ΔT. This may be a demerit of *Method* (B). Note also that though

Method (*B*) is simpler in form, its applicability is narrower than *Method* (*A*); for example, *Method* (*B*) cannot be applied to the study of diatomic interactions.

Acknowledgment. Part of this study has been supported by a Grant-in-Aid for Scientific Research from the Ministry of Education of Japan.

References

1. Koga, T.: Theoret. Chim. Acta (Berl.), **58**, 173 (1981)
2. Dirac, P. A. M.: The principles of quantum mechanics, 4th ed. London: Oxford U.P. 1958
3. Clinton, W. L.: J. Chem. Phys. **33**, 1603 (1960)
4. Hurley, A. C.: Proc. Roy. Soc. London, **A226**, 170 (1954); J. Chem. Phys. **37**, 449 (1962)
5. Nalewajski, R. F.: Chem. Phys. Lett. **54**, 502 (1978); Intern. J. Quantum Chem. **S12**, 87 (1978)
6. Goodisman, J.: Diatomic interaction potential theory. Vol. 1. Fundamentals. New York: Academic Press 1973
7. Koga, T., Morita, M.: Theoret. Chim. Acta (Berl.) **59**, 639 (1981)
8. Epstein, S. T., Hurley, A. C., Wyatt, R. E., Parr, R. G.: J. Chem. Phys. **47**, 1275 (1967)
9. McKinley, W. A.: Am. J. Phys. **39**, 905 (1971); Garcia-Sucre, M.: J. Chem. Phys. **67**, 579 (1977); Bertlmann, R. A., Ono, S.: Phys. Lett. **96B**, 123 (1980)
10. Koga, T., Morita, M.: Theoret. Chim. Acta (Berl.), **59**, 423 (1981)
11. Koga, T., Sugawara, M., Morita, M.: Theoret. Chim. Acta (Berl.) in press
12. Nelander, B.: J. Chem. Phys. **51**, 469 (1969); Srebrenik, S., Messer, R.: J. Chem. Phys. **63**, 2768 (1975); Epstein, S. T.: The variational method in quantum chemistry, New York: Academic 1974
13. Cooper, M. J.: Adv. Phys. **20**, 453 (1971); Contemp. Phys. **18**, 489 (1977)
14. Epstein, I. R.: Acc. Chem. Res. **6**, 145 (1973); in: International review of science. Physical chemistry. Ser. 2. Vol. 1. Buckingham, A. D., Coulson, C. A., ed. London: Butterworths 1975
15. Williams, B. G., ed.: Compton scattering. New York: McGraw-Hill 1977
16. Parr, R. G., Brown, J. E.: J. Chem. Phys. **49**, 4849 (1968)
17. Takahata, Y., Parr, R. G.: Chem. Phys. Lett. **4**, 109 (1969)
18. Walsh, A. D.: J. Chem. Soc. 2260, 2266 (1953)
19. Coulson, C. A.: Mol. Phys. **26**, 507 (1973)
20. Conroy, H.: J. Chem. Phys. **51**, 3979 (1969); Shoucri, R. M., Darling, B. T.: J. Chem. Phys. **56**, 1789 (1972); Hernandez, J. A., Carbo, R.: J. Chem. Phys. **62**, 2637 (1975)
21. Conroy, H.: J. Chem. Phys. **40**, 603 (1964)
22. Sneddon, I. N.: Fourier transforms. New York: McGraw-Hill 1951; Kaijser, P., Smith, Jr., V. H.: Adv. Quantum Chem. **10**, 37 (1977)

Received September 17, 1981